HHS Public Access

Author manuscript

J Surg Res. Author manuscript; available in PMC 2022 August 01.

Published in final edited form as:

J Surg Res. 2021 August ; 264: 327–333. doi:10.1016/j.jss.2021.02.022.

A novel color-coded liver metastasis mouse model to distinguish tumor and adjacent liver segment

Hiroto Nishino, MD, PhD[a,b,c,d], **Hannah M. Hollandsworth, MD**[a,b], **Siamak Amirfakhri, PhD, DVM**[a,b], **Yoshihiko Tashiro, MD, PhD**[a,c], **Jun Yamamoto, MD**[a,c], **Michael Turner, MD**[a,b], **Thinzar M. Lwin, MD, MS**[a,b], **Bernhard B. Singer, PhD**[e], **Robert M. Hoffman, PhD**[a,b,c], **Michael Bouvet, MD**[a,b]

[a.]Department of Surgery, University of California San Diego, San Diego, CA, USA

[b.]Department of Surgery, VA San Diego Healthcare System, San Diego, CA, USA

[c.]AntiCancer, Inc., San Diego, CA, USA

[d.]Department of Surgery, Graduate School of Medicine, Kyoto University, Kyoto, Japan

[e.]Institute of Anatomy, Medical Faculty, University of Duisburg-Essen, Essen, Germany

Abstract

Background: It is difficult to distinguish between a tumor and its liver segment with traditional use of indocyanine green (ICG) alone. In the present study, a method was used to limit ICG to the adjacent liver segment and a spectrally-distinct fluorescently-labeled tumor-specific antibody against human carcinoembryonic antigen-related cell-adhesion molecules (CEACAMs) was used to label the metastatic tumor in a patient-derived orthotopic xenograft (PDOX) mouse model to enable color-coded visualization of colon-cancer liver metastases with its adjacent liver segment.

Materials and Methods: Nude mice received surgical orthotopic implantation of colon-cancer liver metastases derived from two patients. An anti-CEACAM monoclonal antibody (mAb 6G5j) was conjugated to a near-infrared dye IR700DX (6G5j-IR700DX). After three weeks, mice received 6G5j-IR700DX via tail-vein injection 48 hours before surgery. ICG was intravenously injected after ligation of the left or left lateral Glissonean pedicle resulting in labeling of the segment with preserved blood-flow in the liver. Imaging was performed with the Pearl Trilogy and FLARE Imaging Systems.

Corresponding author Michael Bouvet, MD, UCSD Moores Cancer Center, 3855 Health Sciences Drive #0987, La Jolla, CA, 92093-0987, mbouvet@ucsd.edu, Phone: +1-858-822-6191, Fax: +1-858-822-6192.

AUTHOR CONTRIBUTIONS

All authors were involved in conception and design of the study. HN, HMH and SA were involved in the acquisition of the data. HN, YT, JY, MT, TML and MB were involved in analysis and interpretation of data. HN and HMH were involved in drafting of the manuscript. All authors were involved in critical revision of the manuscript for important intellectual content. All authors gave final approval of the version to be submitted. All authors agree to be accountable for all aspects of the work, ensuring that questions related to the accuracy or integrity of any part of the work are appropriately investigated and resolved.

DECLARATION OF INTERESTS

HN, YT, JY, and RMH are non-salaried affiliates of AntiCancer, Inc. The other authors report no proprietary or commercial interest in any product mentioned or concept discussed in this article.

Results: The metastatic liver tumor had a clear fluorescence signal due to selective tumor targeting by 6G5j-IR700DX, which was imaged on the 700 nm channel. The adjacent liver segment with preserved blood-flow in the liver had a clear fluorescence ICG 800 nm signal, while the left or left lateral segment had no fluorescence signal. Overlay of the images showed clear color-coded differentiation between the tumor labeled as 700 nm and the liver segment labeled at 800 nm.

Conclusions: Color-coding of the tumor and uninvolved liver segment has the potential for an optimal liver resection.

Keywords

Liver metastases; Colon cancer; Nude mouse model; Indocyanine green; Fluorescent tumor-specific antibody; CEACAM

INTRODUCTION

Liver surgery offers the chance for long-term survival and is the only potentially curative therapy for patients with colorectal liver metastases (1). There are two main procedures for liver surgery: one is partial liver resection for securing the surgical margin and the other is anatomic liver resection, which is based on the portal flow (2). In the treatment of colorectal liver metastases, negative (≥ 1 mm) surgical margin is the present standard (3) while anatomic liver resection of the cancer-bearing portal territory is recommended for the treatment of hepatocellular carcinoma (4). Partial liver resection is selected to obtain negative surgical margin with parenchymal sparing hepatectomy for preservation of an adequate functional liver remnant (5). On the other hand, anatomic liver resection is chosen depending on the number of tumors and the location of the major vessels such as two-stage hepatectomy for bilateral colorectal liver metastasis cases (6).

Indocyanine green (ICG) has been developed in the field of liver surgery to label liver segments or liver metastases (7). Pre-operative ICG administration provides tumor location for partial liver resection (8). Small colon cancer liver metastases have previously been identified by ICG fluorescence in an orthotopic nude mouse models (9). Intra-operative ICG administration can demarcate liver segments for anatomic liver resection (10). We have improved the specificity of liver segment labeling with ICG after the ligation of the Glissonean pedicle in a mouse model (11). However, it still may be difficult to distinguish between tumor and liver segments, especially when the tumor lies close to a fluorescent liver segment (12).

We have previously demonstrated that a carcinoembryonic antigen-related cell-adhesion molecule (CEACAM) fluorescent antibody can specifically detect primary and metastatic colon cancer in mouse models (13). Our aim in this study was to develop a color-coded fluorescent labeling to provide a distinct boundary between tumor and the adjacent liver segment using a spectrally-distinct fluorescently-labeled tumor-specific antibody in combination with ICG. using a patient-derived orthotopic xenograft (PDOX) nude mouse models (14).

MATERIALS AND METHODS

Nude Mice

Nude (nu/nu) mice, age 4–6 weeks purchased from Jackson Lab (Bar Harbor, ME, USA), were used for this study. The animals were fed an autoclaved laboratory diet. All surgical procedures were performed with anesthesia by intra-muscular injection of ketamine, xylazine and acepromazine reconstituted in phosphate-buffered saline (PBS). Mice were treated with buprenorphine for pain control after surgical procedures. At the conclusion of the study, mice were euthanized with CO_2 inhalation, which was confirmed with cervical dislocation. All studies were approved by the San Diego Veterans Administration Medical Center Institutional Animal Care and Use Committee (IACUC, animal use protocol A17–020).

Antibody-fluorophore conjugation

Anti-CEACAM monoclonal antibody (6G5j: B.B.Singer, Institute for Anatomy, Essen, Germany) was conjugated to near-infrared dye IR700DyeDX NHS ester (LI-COR Biosciences Inc., Lincoln, NE, USA) (6G5j-IR700DX), per methods previously described (13).

Subcutaneous patient-derived orthotopic xenografts with tumors

Two human patient colon cancer liver metastases (CM2 and Liver5) were established under sterile conditions using previously described procedures (13).

Sutureless surgical orthotopic implantation (SOI) of a patient-derived colon cancer liver metastasis

The procedure of sutureless surgical orthotopic implantation (SOI) was previously described (15). Briefly, a 10 mm incision was made vertically in the midline of the upper abdomen through the skin and peritoneum. After removal of the xyphoid process, the left lobe of the liver was exposed. A single 1 mm^3 tumor fragment was implanted into the left lobe of the liver without any suturing. The left lobe of the liver was returned to the abdominal cavity and the skin and peritoneum were closed with 6–0 surgical sutures. Six mice were implanted with CM2 and four were implanted with Liver5.

Administration of fluorescent agents

Three weeks after SOI, mice were administered 50 μg of 6G5j-IR700DX via tail vein injection. Forty-eight hours later, ICG was administered as previously described, by exposing the liver and ligating the left Glissonean pedicle as previously described (11). A schematic diagram of the experimental protocol is shown in Figure 1.

In vivo imaging

Mice were anesthetized prior to imaging and laparotomy was performed to expose the liver. For 700 nm and 800 nm intra-vital static imaging, the Pearl Trilogy Small Animal Fluorescence Imaging System (LI-COR, Lincoln. NE, USA) was used. For intra-vital dynamic imaging the FLARE Imaging System (Curadel, MA, USA) was used.

Statistical analysis

Imaging analysis was performed using Image Studio Software Small Animal Imaging Analysis (LI-COR, Lincoln, NE) and statistical analysis was performed using SAS software (JMP 14.2.0; SAS Institute Inc., Cary, NC). Continuous variables were expressed as mean ± standard deviation. The liver was set as the background and an area of interest around the tumor fluorescence was automatically provided by the system with a minimum of 250 pixels and at least 2.5 standard deviations from the background signal. Tumor-to-liver ratio (TLR) was calculated for each mouse by dividing maximum tumor fluorescence by maximum liver fluorescence. Mean TLR was determined for the entire cohort.

RESULTS

In vivo Imaging

Six nude mice underwent liver SOI of CM2 and four received liver SOI of Liver5 human patient derived colon cancer liver metastases. Images were acquired with the Pearl Trilogy Small Animal Imaging System 48 hours after 6G5j-IR700DX administration via tail vein. The CM2 mice tumor expressed 700 nm signal (red pseudo-color) and representative images of 2 cases are shown in Figure 2A and 2C. Images were then acquired a few minutes after ICG administration via tail vein. The CM2 mice tumor expressed 700 nm signal (red pseudo-color) and the area with preserved blood flow of the liver expressed 800 nm signal (green pseudo-color). Figure 2B and 2D show the anatomical position and cranial inversion of the liver in the same mouse as Figure 2A and Figure 2C, respectively. There was minimal variation in fluorescence level between mice. The TLR of each mouse is shown in Figure 3 and the mean TLR for the entire cohort of mice was 4.40 ± 0.96.

The Liver5 mice tumor expressed 700 nm signal (red pseudo-color) and expressed 800 nm signal (green pseudo-color) on the area with preserved blood flow of the liver. All four mice had similar fluorescence. The TLR of each mouse is shown in Figure 3 and the mean TLR for the entire cohort of mice was 3.38 + 1.25.

No adverse effects were observed in all cases when anti-CEACAM antibody conjugated to 700 nm dye and ICG were administered concomitantly.

Color-coded labeling with Intra-vital Dynamic Imaging

After confirmation of fluorescence signals with Pearl Trilogy Small Animal Imaging System, imaging was performed on the FLARE Imaging System. On the bright-light channel, the mouse position was carefully aligned (Figure 4A). On the 700 nm channel, the tumor had a clear fluorescence signal of 6G5j-IR700DX with minimal background liver signal (Figure 4B). On the 800 nm channel, the left or left lateral lobe had no fluorescence signal due to ligation of the Glissonean pedicle and the area with preserved blood flow in the liver had the clear fluorescence signal of ICG (Figure 4C). Overlay mode (bright-light, 700 nm and 800 nm) showed clear differentiation between tumor and segmental boundary (Figure 4D).

DISCUSSION

In the present study, we demonstrate that color-coded fluorescence labeling using a fluorescently labeled tumor-specific antibody against human CEACAMs in combination with ICG enhances the visualization of the boundary between the colon-cancer liver metastatic tumor and its adjacent liver segment in PDOX mouse models.

Within the field of liver surgery, the hepatic metabolism of ICG makes it useful for many intraoperative real-time imaging approaches (16). Two of the most important uses of ICG are identifying hepatic tumors and visualizing hepatic segments. Pre-operative administration of ICG has been used for tumor identification. Although it is not highly sensitive or tumor-specific, it can be used to identify the location of tumors using different mechanisms for hepatocellular carcinoma and metastatic liver tumor (8). ICG is used to help ensure a negative surgical margin in liver resection (17). In addition to tumor labelling, ICG has been used to identify liver segments as during anatomic liver resection, which is associated with a higher risk of fatal complications due to the lack of visibility of intrahepatic structures (10). This approach takes advantage of the fact that ICG entering via the portal vein remains in the hepatocyte for several hours and is excreted into the bile duct (18). In recent years, this technique has been applied to real-time navigation for continuous guidance of the transection plane in anatomic liver resection (12, 19, 20). Depending on the location of the tumor, there are often situations when both of these techniques could be used, but there is no way to visually distinguish between them.

Anatomic resection is based on portal flow from an oncological perspective, and there are two main methods of ICG administration: positive staining and negative staining (21). In positive staining, the fluorescent area is resected, and the non-fluorescent area is resected in negative staining. In patients with tumors receiving blood supply by two or more portal veins, the multiple staining method is useful (22). We used the negative staining method with Glissonean sheath ligation, which is easy to perform and highly reproducible in mouse models (11).

In our recent study (13), 6G5j-IR800CW injection did not immunohistochemically stain human colon and western blotting of 6G5j-IR800CW for CEACAM expression showed low expression in normal human colon and no expression in normal mice colon. It was also shown that of two human colon cancer cell lines and 14 patient-derived colon cancers surgically obtained at our hospital, only the HCT116 human colon cancer cell line did not express CEACAM. Jantscheff et al. reported that 95.9% of patients showed enhanced expression in at least one of CEACAM 1, CEACAM5 and CEACAM6 molecules in 243 patients (23). We selected two patient tumors with high pre-operative CEA for establishment of PDOX mouse models based on the results of whole membrane western blotting of CEACAM expression in colon-cancer lysates (13). We selected tumor-specific antibody conjugated to 700 nm dye as a fluorophore for the tumor visualization since this dye has a distinctly different wavelength than ICG.

There are several limitations in this study. First, there is a lack of information on CEACAM expression percentage of liver metastases and normal liver tissue. With regard to the liver,

overexpression of CEACAM6 in colorectal cancer cells increases invasiveness and correlates with the highest expression of CEACAM6 in colorectal liver metastases (24), but no data has been reported on the percentage of CEACAM expression in liver metastases or normal liver tissue, and further studies are needed. In addition, the segment I or IV resections have a dual blood supply so this technology will be limited in this instance.

Color-coded surgery with multiple color imaging has been demonstrated in previous studies. Yano et al developed color-coded FGS with green fluorescent protein (GFP)-labeled cancer cells and red fluorescent protein (RFP)-labeled stroma cells in a PDOX mouse model of pancreatic cancer (25). Color-coded FGS was more effective than BLS or single-color FGS to prevent recurrence in the model. In the clinical field of neurosurgery, dual labeling with 5-ALA for distinguishing tumor and fluorescein for providing tissue fluorescence of adjacent brain tissue has been reported (26).

Color-coded surgery using multiple wavelength filters is promising for further advances in navigation surgery, such as viewing the boundaries of tumors, background tissues, blood vessels and nerves (27, 28). The results shown in the present study indicated that the signals at 700 nm and 800 nm could be clearly recognized, and the overlay with the bright field was also favorable for liver surgery in mouse models. Especially in laparoscopic or robotic surgery, which has made remarkable progress in recent years, it is easy to perform intra-operative merged imaging, so it is possible to reproduce this technique in clinical applications. These advances are useful for anatomic liver resection cases in which the tumor is located close to the boundary of the liver segments and expected to lead to safer and more reliable tumor resections and fewer complications.

The present proof-of-principle study demonstrate that metastatic liver tumor and adjacent liver segment can be readily distinguished offers suggestions that could lead to further advances in navigation liver surgery.

CONCLUSIONS

This study shows that the combination of ICG (800 nm) and anti-CEACAM antibody conjugated to 700 nm dye distinguish the tumor and the liver segment in which it resides and has potential for FGS of colorectal cancer liver metastases.

ACKNOWLEDGEMENTS

This study was funded by Veterans Affairs Merit Review grant numbers 1 101 BX003856–01A1 and 1 101 BX004494–01 (MB), NIH/NCI T32CA121938 (HH and TML), and The Yasuda Medical Foundation (HN).

REFERENCES

1. Adam R, De Gramont A, Figueras J, Guthrie A, Kokudo N, Kunstlinger F, Loyer E, Poston G, Rougier P, Rubbia-Brandt L, Sobrero A, Tabernero J, Teh C, Van Cutsem E, and Jean-Nicolas Vauthey E. g. The oncosurgery approach to managing liver metastases from colorectal cancer: a multidisciplinary international consensus. Oncologist 17: 1225–1239, 2012. [PubMed: 22962059]
2. Makuuchi M, Hasegawa H, and Yamazaki S Ultrasonically guided subsegmentectomy. Surg Gynecol Obstet 161: 346–350, 1985. [PubMed: 2996162]

3. Hamady ZZ, Lodge JP, Welsh FK, Toogood GJ, White A, John T, and Rees M One-millimeter cancer-free margin is curative for colorectal liver metastases: a propensity score case-match approach. Ann Surg 259: 543–548, 2014. [PubMed: 23732261]
4. Hasegawa K Kokudo N., Imamura H, Matsuyama Y, Aoki T, Minagawa M, Sano K, Sugawara Y, Takayama T, and Makuuchi M Prognostic impact of anatomic resection for hepatocellular carcinoma. Ann Surg 242: 252–259, 2005. [PubMed: 16041216]
5. Mise Y, Aloia TA, Brudvik KW, Schwarz L, Vauthey JN, and Conrad C Parenchymal-sparing Hepatectomy in Colorectal Liver Metastasis Improves Salvageability and Survival. Ann Surg 263: 146–152, 2016. [PubMed: 25775068]
6. Adam R, Laurent A, Azoulay D, Castaing D, and Bismuth H Two-stage hepatectomy: A planned strategy to treat irresectable liver tumors. Ann Surg 232: 777–785, 2000. [PubMed: 11088072]
7. Majlesara A, Golriz M, Hafezi M, Saffari A, Stenau E, Maier-Hein L, Muller-Stich BP, and Mehrabi A Indocyanine green fluorescence imaging in hepatobiliary surgery. Photodiagnosis Photodyn Ther 17: 208–215, 2017. [PubMed: 28017834]
8. Ishizawa T, Fukushima N, Shibahara J, Masuda K, Tamura S, Aoki T, Hasegawa K, Beck Y, Fukayama M, and Kokudo N Real-time identification of liver cancers by using indocyanine green fluorescent imaging. Cancer 115: 2491–2504, 2009. [PubMed: 19326450]
9. Tashiro Y, Hollandsworth HM, Nishino H, Yamamoto J, Amirfakhri S, Filemoni F, Sugisawa N, Aoki T, Murakami M, Hoffman RM, and Bouvet M Indocyanine Green Labels an Orthotopic Nude-Mouse Model of Very-Early Colon-Cancer Liver Metastases. In Vivo 34: 2277–2280, 2020. [PubMed: 32871750]
10. Aoki T, Yasuda D, Shimizu Y, Odaira M, Niiya T, Kusano T, Mitamura K, Hayashi K, Murai N, Koizumi T, Kato H, Enami Y, Miwa M, and Kusano M Image-guided liver mapping using fluorescence navigation system with indocyanine green for anatomical hepatic resection, World J Surg 32: 1763–1767, 2008. [PubMed: 18543027]
11. Nishino H, Hollandsworth HM, Tashiro Y, Yamamoto J, Amirfakhri S, Filemoni F, Sugisawa N, Hoffman RM, and Bouvet M Ligation Method to Specifically Label a Liver Segment With Indocyanine Green in an Orthotopic Nude-Mouse Liver-Metastasis Model. In Vivo 34: 3159–3162, 2020. [PubMed: 33144419]
12. Nishino H, Hatano E, Seo S, Nitta T, Saito T, Nakamura M, Hattori K, Takatani M, Fuji H, Taura K, and Uemoto S Real-time Navigation for Liver Surgery Using Projection Mapping With Indocyanine Green Fluorescence: Development of the Novel Medical Imaging Projection System. Ann Surg 267: 1134–1140, 2018. [PubMed: 28181939]
13. Hollandsworth HM, Amirfakhri S, Filemoni F, Schmitt V, Wennemuth G, Schmidt A, Hoffman RM, Singer BB, and Bouvet M Anti-carcinoembryonic antigen-related cell adhesion molecule antibody for fluorescence visualization of primary colon cancer and metastases in patient-derived orthotopic xenograft mouse models. Oncotarget 11: 429–439, 2020. [PubMed: 32064046]
14. Hoffman RM Patient-derived orthotopic xenografts: better mimic of metastasis than subcutaneous xenografts. Nat Rev Cancer 15: 451–452, 2015. [PubMed: 26422835]
15. Nishino H, Hollandsworth HM, Sugisawa N, Yamamoto J, Tashiro Y, Inubushi S, Hamada K, Sun YU, Lim H, Amirfakhri S, Filemoni F, Hoffman RM, and Bouvet M Sutureless Surgical Orthotopic Implantation Technique of Primary and Metastatic Cancer in the Liver of Mouse Models. In Vivo 34: 3153–3157, 2020. [PubMed: 33144418]
16. Lwin TM, Hoffman RM, and Bouvet M Fluorescence-guided hepatobiliary surgery with long and short wavelength fluorophores. Hepatobiliary Surg Nutr 9: 615–639, 2020. [PubMed: 33163512]
17. Aoki T, Koizumi T, Mansour DA, Fujimori A, Kusano T, Matsuda K, Nogaki K, Tashiro Y, Hakozaki T, Wada Y, Shibata H, Tomioka K, Hirai T, Yamazaki T, Saito K, Enami Y, Koike R, Mitamura K, Yamada K, Watanabe M, Otsuka K, and Murakami M Virtual reality with three-dimensional image guidance of individual patients' vessel anatomy in laparoscopic distal pancreatectomy. Langenbecks Arch Surg 405: 381–389. 2020. [PubMed: 32410077]
18. Cusin F, Fernandes, Azevedo L, Bonnaventure R, Desmeules J, Daali Y, and Pastor CM Hepatocyte Concentrations of Indocyanine Green Reflect Transfer Rates Across Membrane Transporters. Basic Clin Pharmacol Toxicol 120: 171–178, 2017. [PubMed: 27623731]

19. Terasawa M, Ishizawa T, Mise Y, Inoue Y, Ito H, Takahashi Y, and Saiura A Applications of fusion-fluorescence imaging using indocyanine green in laparoscopic hepatectomy. Surg Endosc 31: 5111–5118, 2017. [PubMed: 28455774]

20. Nishino H, Seo S, Hatano E, Nitta T, Morino K, Toda R, Fukumitsu K, Ishii T,, Taura K, and Uemoto S. What is a precise anatomic resection of the liver? Proposal of a new evaluation method in the era of fluorescence navigation surgery. J Hepatobiliary Pancreat Sci 2020, in press

21. Ishizawa T, Bandai Y, and Kokudo N Fluorescent cholangiography using indocyanine green for laparoscopic cholecystectomy: an initial experience. Arch Surg 144: 381–2, 2009. [PubMed: 19380655]

22. Kobayashi Y, Kawaguchi Y, Kobayashi K, Mori K, Arita J, Sakamoto Y, Hasegawa K, and Kokudo N Portal vein territory identification using indocyanine green fluorescence imaging: Technical details and short-term outcomes. J Surg Oncol. 116: 921–931,2017. [PubMed: 28695566]

23. Jantscheff P, Terracciano L, Lowy A, Glatz-Krieger K, Grunert F, Micheel B, Briimmer J, Laffer U, Metzger U, Herrmann R, and Rochlitz C Expression of CEACAM6 in resectable colorectal cancer: a factor of independent prognostic significance. J Clin Oncol 21: 3638–46, 2003. [PubMed: 14512395]

24. Kim KS, Kim JT, Lee SJ, Kang MA, Choe IS, Kang YH, Kim SY, Yeom YI, Lee YH, Kim JH, Kim KH, Kim CN,Kim JW, Nam MS, and Lee HG Overexpression and clinical significance of carcinoembryonic antigen-related cell adhesion molecule 6 in colorectal cancer. Clinica Chimica Acta 415, 12–19, 2013.

25. Yano S, Hiroshima Y, Maawy A, Kishimoto H, Suetsugu A, Miwa S, Toneri M, Yamamoto M, Katz MH, Fleming JB, Urata Y, Tazawa H, Kagawa S, Bouvet M,, Fujiwara T, and Hoffman RM Color-coding cancer and stromal cells with genetic reporters in a patient-derived orthotopic xenograft (PDOX) model of pancreatic cancer enhances fluorescence-guided surgery. Cancer Gene Ther 22: 344–350, 2015. [PubMed: 26088297]

26. Suero Molina E, Wolfer J, Ewelt C, Ehrhardt A, Brokinkel B, and Stummer W Dual-labeling with 5-aminolevulinic acid and fluorescein for fluorescence-guided resection of high-grade gliomas: technical note. J Neurosurg 128: 399–405, 2018. [PubMed: 28338432]

27. Ishizawa T, and Kokudo N The beginning of a new era of digestive surgery guided by fluorescence imaging. Liver Cancer 3: 6–8, 2014. [PubMed: 24804172]

28. Walsh EM, Cole D, Tipimeni KE, Bland KI, Udayakumar N, Kasten BB, Bevans SL, McGrew BM, Kain JJ, Nguyen QT, Rosenthal EL, and Warram JM Fluorescence Imaging of Nerves During Surgery. Ann Surg 270: 69–76, 2019. [PubMed: 30649014]

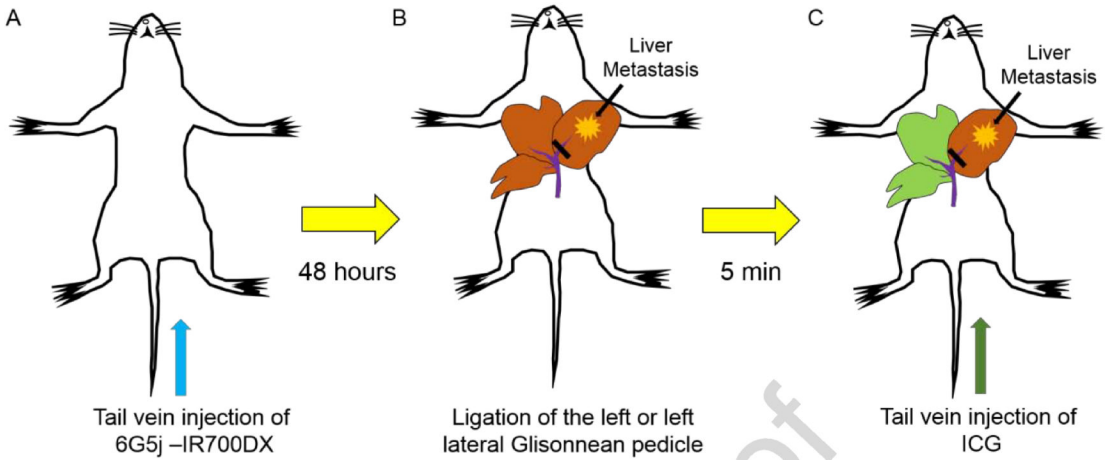

Figure 1.

Administration of indocyanine green (ICG) and anti-CEACAM monoclonal antibody (6G5j) fluorescent antibody. A) 50 μg of 6G5j conjugated to near-infrared dye IR700DyeDX NHS ester was injected via tail vein. B) Isolation and ligation of the left Glissonean pedicle or left lateral Glissonean pedicle during surgery was performed. C) 10 μg of ICG was injected via tail vein resulting in labeling of the area with preserved blood flow in the liver.

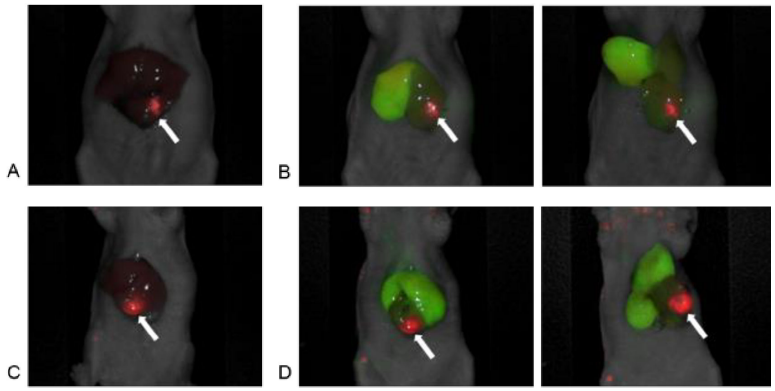

Figure 2.

In vivo imaging using the Pearl Trilogy Small Animal Imaging System. A) A representative image of red pseudo-color based on 700 nm signal of anti-CEACAM monoclonal antibody (6G5j) targeting surgically orthotopically implanted CM2 colon cancer liver metastatic patient tumor. Tumor-to-liver ratio (TLR) was 5.84. B) Red pseudo-color based on 700 nm signal of 6G5j targeting CM2 tumor and green pseudo-color based on 800 nm signal of ICG targeting the right lobe in the liver. Anatomic position and cranial inversion of the liver in the same mouse as Figure 2A were shown. C) Another representative image of red pseudo-color based on 700 nm signal of 6G5j targeting CM2 tumor. Tumor-to-liver ratio (TLR) was 3.88. D) Red pseudo-color based on 700 nm signal of 6G5j targeting CM2 tumor and green pseudo-color based on 800 nm signal of ICG targeting the right and the left medial lobe in the liver. Anatomic position and cranial inversion of the liver in the same mouse as Figure 2B were shown, (arrow: liver metastatic tumor)

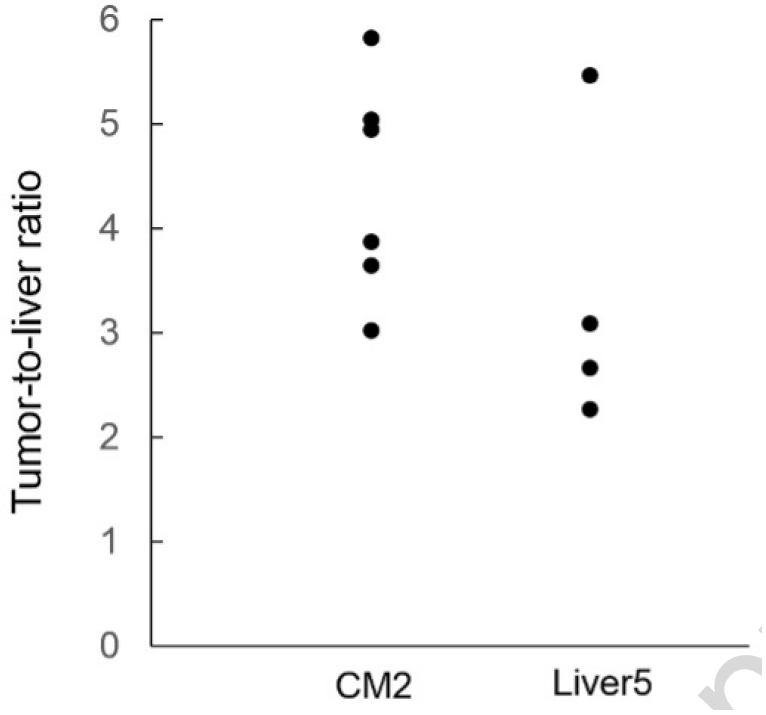

Figure 3.

The dot chart of tumor-to-liver ratio (TLR). TLR was calculated for each mouse by dividing maximum tumor fluorescence by maximum liver fluorescence. In CM2 cohort, the mean TLR was 4.40 ± 0.96. In Liver5 cohort, the mean TLR for the entire cohort of mice was 3.38 ± 1.25.

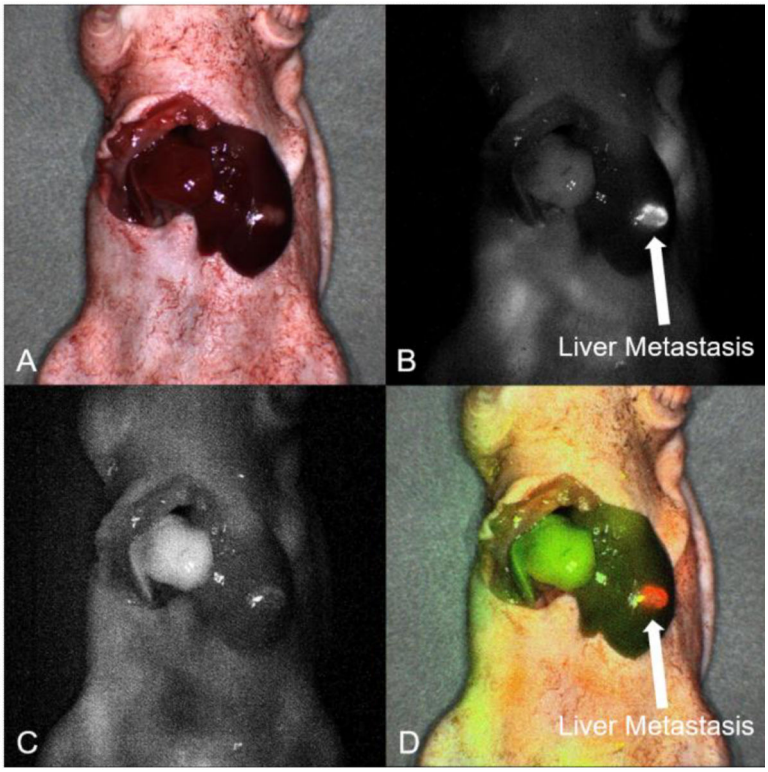

Figure 4.

Intra-vital dynamic imaging using the FLARE Imaging System. A) On the bright-light channel, the mice position was aligned. B) On the 700 nm channel, the surgically orthotopically implanted Liver5 colon cancer liver metastatic patient tumor had a clear fluorescence signal of anti-CEACAM monoclonal antibody (6G5j). (arrow: liver metastatic tumor). C) On the 800 nm channel, the left lobe had no fluorescence signal due to ligation of the left Glissonean pedicle and the right lobe in the liver had the clear fluorescence signal of ICG. D) Overlay mode showed clear differentiation between the tumor and segmental boundary on the same image, (arrow: liver metastatic tumor).